Research Square

Preprints are preliminary reports that have not undergone peer review.
They should not be considered conclusive, used to inform clinical practice,
or referenced by the media as validated information.

Assessment of Metabolites in Sera and Cerebrospinal Fluids of Rabies-Infected Dogs (Nigeria)

Ukamaka Uchenna Eze

ukamakauchenna.eze@unn.edu.ng

University of Nigeria

Monique Opperman

North-West University

Kenneth Ikejiofor Ogbu

National research institue, Vom

Elmarie Davoren

North-West University

Ernest C Ngoepe

Agricultural Research Council of South Africa

Romanus C Ezeokonkwo

University of Nigeria

Boniface M Anene

University of Nigeria

Livio E Heath

Agricultural Research Council of South Africa

Ilse Du Preez

North-West University

Claude T Sabeta

University of Pretoria

Research Article

Keywords: Rabies, Dogs, Antemortem diagnosis, Differential Metabolites, Metabolomics

Posted Date: March 9th, 2026

DOI: https://doi.org/10.21203/rs.3.rs-9010194/v1

License: This work is licensed under a Creative Commons Attribution 4.0 International License.
Read Full License

Additional Declarations: No competing interests reported.

Abstract

Introduction: Rabies remains a neglected zoonotic disease of global public health importance due to its near-universal fatality, lack of reliable preclinical diagnostics, and absence of effective treatment after symptom onset.

Methodology: This study investigated early metabolic alterations associated with rabies virus infection by profiling serum and cerebrospinal fluid (CSF) metabolites in naturally infected dogs during the incubation phase. A total of 231 samples (brain tissue, serum, and CSF) were obtained from dogs slaughtered for human consumption in southeastern and north-central Nigeria.

Results: Rabies antigen was detected in brain tissues using the direct fluorescent antibody test, identifying 20 positive cases (8.7%). Corresponding serum and CSF samples were classified as rabies-positive, while 20 negative samples were selected for comparison. Untargeted metabolomic analysis was performed using comprehensive two-dimensional gas chromatography coupled with time-of-flight mass spectrometry (GC×GC-TOFMS). Data processing included contaminant removal, normalization, batch correction, and scaling, followed by multivariate, univariate, pathway enrichment, and ROC analyses. The serum dataset yielded 868 retained compounds, while 300 compounds were retained from CSF after quality control. Missing data did not differ significantly between groups. Pathway analysis revealed significant perturbations in glycerolipid metabolism, glyoxylate and dicarboxylate metabolism, the pentose phosphate pathway, and amino acid metabolism in serum. Four serum metabolites remained significant after correction, with an unannotated compound (Analyte 634) showing strong discriminatory ability (AUC = 0.962). CSF analysis indicated enrichment in pentose phosphate, glutathione, and nicotinate metabolism. Indolelactic acid was consistently downregulated in both matrices. One shared metabolite was detected in serum and CSF.

Conclusion: Overall, the findings demonstrate early metabolic disturbances during rabies infection and identify potential biomarkers for preclinical detection

1. Introduction

Rabies is an invariably fatal zoonotic disease known for thousands of years for which prevention remains the most cost-effective control measure (WHO, 2024). Most developed countries have eliminated dog-mediated rabies through strategic and targeted vaccination programs. However, achieving similar success in many low- and middle-income countries has proven to be a huge challenge, despite the tripartite's (World Health Organization, World Organization for Animal Health and Food and Agricultural Organization) goal of global rabies elimination by 2030 (WHO, 2018). In Nigeria, beyond the challenges and barriers of vaccine cost and its limited availability in the needy rural communities, irresponsible dog ownership continues to play a critical role in sustaining rabies endemicity (Atuman et al., 2014; Akanbi et al., 2023). Dogs frequently roam freely during the day and return to their owner's households only at night. This practice of keeping dogs, facilitates rabies transmission among dogs and, subsequently, to humans, particularly children under 15 years of age (Hampson et al., 2015). As a result,

dog-mediated human rabies remains a serious public health problem in rural areas, yet the disease is grossly underreported, with only 998 human and 273 suspected canine rabies cases officially documented across Nigeria between 2017 and 2022 (Abubakar et al., 2024)

There is currently no treatment for rabies. Following the bite of a suspected rabid dog, the recommended intervention is post-exposure prophylaxis (PEP) using rabies immunoglobulin (RIG) and anti-rabies vaccine, which effectively prevents disease progression if administered promptly. However, in many rural parts of Nigeria, the high cost and limited accessibility of PEP often result in preventable deaths (Conceição and Abreu, 2021). Victims and their families frequently assume that the biting dog may not be rabid and, due to financial constraints, resort to cheaper local herbal remedies instead (Mshelbwala et al., 2021; Eugene et al., 2025). The average cost of a full PEP regimen is approximately USD 40, whereas the average daily income of many Nigerians is only USD 1–2, making access to life-saving prophylactic post-exposure vaccination unattainable for much of the rural population (Hampson et al., 2015; WHO, 2018; Eze et al., 2020). Ideally, distinguishing between bites from rabid and non-rabid dogs would reduce unnecessary PEP administration; however, the pathophysiology of rabies complicates this distinction. The causative agent, *Lyssavirus rabies*, along with 18 other species of the *Lyssavirus* genus, evades the host immune system, rendering antemortem diagnosis difficult. Consequently, rabies is typically confirmed only after the onset of clinical signs, at which point the disease is invariably fatal (Rupprecht, 1996; Fooks and Jackson, 2020; ICTV, 2025).

Considering these challenges, novel diagnostic approaches are urgently needed, and metabolomics, one of the emerging “omics” technologies, has shown great promise in clinical diagnostics of infectious diseases (Tounta et al., 2021). Several pathological conditions have resulted in the disturbance of metabolic pathways, often triggered by an imbalance in metabolites either through excessive accumulation or deficiency that compromises normal cellular processes (Qiu et al., 2023). Metabolomic profiling of biofluids, particularly cerebrospinal fluid (CSF), has proven valuable in identifying reliable biomarkers of central nervous system (CNS) diseases such as meningitis, amyotrophic lateral sclerosis, and multiple sclerosis (Coen et al., 2005; Sinclair et al., 2010; Blasco *et al.*, 2011, Hartonen et al., 2013). Since CSF is partially derived from CNS interstitial fluid, its composition closely reflects brain metabolic processes. Metabolomic analysis of canine serum has been increasingly employed to characterize disease-associated metabolic alterations. This approach has identified distinct metabolite changes in conditions such as hypothyroidism, chronic enteropathies, and toxocariasis (Zheng et al., 2019; Muñoz-Prieto et al., 2021; Walker et al., 2022), underscoring its potential as a diagnostic and pathophysiological tool in veterinary medicine.

Metabolomic studies on rabies virus infection are limited. A recent analysis in rabies-infected rats showed that most altered brain metabolites were associated with nucleotide and amino acid metabolism, with aminoacyl-tRNA biosynthesis and purine metabolism identified as the most significantly affected pathways (Zhao et al., 2020). Studies of human CSF infected with rabies has shown that rabies virus infection results in altered metabolism, including a deficiency of tetrahydrobiopterin (BH_4) and monoamine neurotransmitters, and an increase in lactic acid in CSF

(Warrell et al., 1976; Willoughby et al., 2009). CSF lactic acidosis and vasospasm have also been reported (Lamas et al., 1980; Willoughby et al., 2008).

Although several studies have investigated metabolomic changes associated with rabies virus infection, these have primarily been conducted in laboratory animals or in dogs that had already succumbed to the disease (Zhao et al., 2020). To the best of our knowledge, no metabolomic studies have examined rabies-positive dogs that were not yet exhibiting clinical signs. In this study, we utilized the cultural practice of dog meat consumption in Nigeria to obtain samples from apparently healthy dogs destined for slaughter. This allowed us to identify differentially abundant metabolites in rabies-positive dogs prior to the onset of clinical signs. Such metabolites may serve as potential biomarkers for antemortem diagnosis of rabies in dogs, which is critical given that current diagnoses are often tentative once clinical signs appear, by which point the disease is almost invariably fatal, and confirmation can only be made postmortem.

2. Materials and Methods

2.1. Ethical Approval

This study was conducted in strict compliance with international and national ethical standards for animal research. All experimental protocols were reviewed and approved on 28 March 2023 by the Institutional Animal Care and Use Committee (IACUC) of the Faculty of Veterinary Medicine, University of Nigeria, Nsukka (Approval No: FVM-UNN-IACUC-2023-03100). Written informed consent (refer to Appendix II of the supplementary information) was obtained from dog traders and dog meat vendors prior to sample collection, ensuring that the procedures aligned with ethical guidelines for the use of animals and animal products in research.

In addition, ethical clearance was obtained from the South African National Department of Agriculture Ethics Committee on 2 September 2024, in accordance with Section 20 of the Animal Diseases Act of 1984 (Act No. 35 of 1984), Reference No: 12/11/1/1/8 (6640KL). This dual approval reflects strict adherence to established international guidelines for animal welfare and ethical scientific practice

2.2. Study Area and Sample Size

Field sampling was conducted within the North-Central and South-East geopolitical zones of Nigeria. These regions were purposely selected because of their large concentration of dog markets, which serve as major hubs for the trade and slaughter of dogs for human consumption. To achieve a balanced regional representation, one state was randomly selected from each zone: Plateau State from the North-Central region and Enugu State from the South-East region. Within each selected state, two large dog markets with high daily slaughter rates were chosen as sampling sites, based on their importance as major sources of dog meat supply.

The required sample size was calculated using the formula provided by Thrusfield *et al.* (2005), with the calculation based on a previously reported prevalence of 8.3% for rabies in apparently healthy dogs in South-East Nigeria (Eze *et al.*, 2018). The formula yielded a minimum sample size of 117 dogs. However, to improve the statistical robustness, reduce sampling error, and enhance the representativeness of the findings across both regions, the sample size was nearly doubled, and a total of 231 dogs were included in the study. Most dogs presented at the market for slaughter were fed homemade diets by their owners. Both puppies and adult dogs were slaughtered. The Basenji was the primary breed slaughtered for human consumption, and all samples analyzed in this study were obtained from this breed.

2.3. Exclusion Criteria

To avoid confounding factors, strict exclusion criteria were applied. Dogs showing clinical signs suggestive of illness, including dullness, excessive salivation (drooling), marked emaciation, ocular or nasal discharge, diarrhoea, or vomiting, were excluded from the study to ensure that only apparently healthy dogs were sampled. This exclusion was particularly important as the focus of the study was to identify metabolomic changes in rabies-infected dogs before the onset of clinical symptoms. Furthermore, dogs that had already been slaughtered before the arrival of the research team at the market were excluded because the health status of the live dogs was not determined.

2.4. Sample Collection and Processing

The dogs were raised in households within the study regions and sold for human consumption, reflecting the cultural significance of consumption of dog meat in these areas. Each dog was assigned a unique identification tag, which was used to label the corresponding sample set, thereby maintaining consistency and traceability throughout the study. A total of 231 dogs were sampled at slaughter across the two selected markets. From each dog, matched samples comprising brain tissue (BT), CSF, and serum were collected.

Immediately after collection, all samples were transported under strict cold chain conditions to the Rabies Unit of the Central Diagnostic Laboratory at the National Veterinary Research Institute (NVRI), Vom, Plateau State, Nigeria. as per the normal in-country procedure. Lyssavirus antigen detection was performed on all BT samples using the Direct Fluorescent Antibody (DFA) test, following the standard protocol described by Dean *et al.* (1996). Of the 231 BT samples analyzed, 20 (8.7%) tested positive for lyssavirus antigen. The CSF and serum samples corresponding to the infected dogs were accordingly categorized as lyssavirus-positive. For comparative purposes, a set of negative controls was assembled. From the lyssavirus-negative dogs, 20 samples were randomly selected for each sample type (CSF and Serum). This created a balanced dataset of positive and negative specimens for the downstream metabolic analyses. All samples, whether positive or negative, were then stored at -20 °C until further laboratory investigations were carried out

For the purpose of this study, CSF and serum were included due to their complementary relevance in metabolomics research. CSF, which is partly derived from interstitial fluid of the central nervous system,

reflects ongoing biochemical changes in the brain and offers potential for antemortem diagnostic biomarker discovery. Serum, on the other hand, provides a systemic overview of host metabolic responses, bridging central and peripheral changes during rabies infection. Together, these sample types provide a holistic view of both central and systemic metabolic alterations associated with rabies.

2.5. Metabolite extraction

The stored positive and negative serum and CSF samples were shipped under cold chain to the BSL-3 facility of the Transboundary Animal Diseases, Agricultural Research Council, Onderstepoort Veterinary Research, South Africa, where initial metabolite extractions were performed.

Serum sample preparation followed a previously described method for application to untargeted metabolomics analyses (Swanepoel *et al.*, 2020), with modifications. For metabolite extraction, 100 µL of 3-phenylbutyric acid (100 ppm, Merck, Darmstadt, Germany) was added to 100 µL of each sample as an internal standard. Proteins were precipitated by the addition of 600 µL ice-cold acetonitrile, followed by incubation on ice for 10 min. The samples were then centrifuged at 8,000 rpm for 8 min at 4 °C, and the resulting supernatants were collected and dried under nitrogen. Metabolite extraction from CSF followed the same protocol as the serum, with three modifications: a smaller volume of CSF was used (50 uL) and methanol (800 uL) replaced acetonitrile as the precipitating solvent.

Serum and CSF extracts were sent on ice to the Centre for Human Metabolomics (CHM), North-West University, South Africa, for further processing and analysis. Extracts were resuspended in 300 uL ice-cold acetonitrile and vortexed, whereafter 200 uL extraction solvent (chloroform:methanol:water (1:3:1)) was added to the samples, followed by another brief vortexing step. Extracts were then centrifuged at 4000 rpm for 10 min (4°C), whereafter the supernatant was collected, transferred to glass vials and dried under nitrogen. The dried extracts were then derivatized with 50 uL of methoxyamine hydrochloride in pyridine (20 mg/mL, Merck) at 55°C for 60 min, and trimethylated with 50 uL of BSTFA containing 1% TMCS (Sigma-Aldrich, St. Louis, Missouri, USA) at 55°C for 60 min. Samples were extracted and derivatized in a random order.

For quality control, each batch included five replicate injections of a fatty acid methyl ester (FAMES) standard mixture, the system blank (no injection), and the extraction blank (full sample preparation but no matrix). All solvents used were ultra-pure Burdick & Jackson brands (Anatech, South Africa).

2.6. GCxGC/TOFMS analyses

Table 1 provides an overview of the comprehensive two-dimensional gas chromatography-time of flight mass spectrometry (GC×GC-TOFMS) operating parameters applied for the analyses.

Table 1: Instrument and software conditions

GCXGC	Agilent 7890A GC (Agilent, Atlanta, GA) equipped with a Gerstel Multi-Purpose Sampler (MPS) (Gerstel GmbH), and a cryogenic cooler.
Injection	1µL with inlet temp 270 °C, split 5:1
Columns	1D: Rxi-5MS, 28.2m x 0.25mm x 0.25µm (Restek) 2D: Rxi-17Sil MS, 1.32m x 0.25mm x 0.25µm (Restek)
Carrier Gas	Helium @ 1 mL/min
Primary oven Program	Initial temp of 70 ^{o}C (2 min) then increased with 4 ^{o}C/min to 300 ^{o}C (2 min hold)
Secondary oven Program	Initial temp of 85 ^{o}C (2 min) then increase with 4.5 ^{o}C/min to 300 ^{o}C (5 min hold)
Modulator Program	Initial temp of 100 ^{o}C (2 min) then increase with 4.5 ^{o}C/min to 310 ^{o}C (12 min hold) Cryo-modulation with hot nitrogen gas pulses (0.5s every 3 s)
Transfer line	270 °C
MS	Pegasus 4D GCxGC-TOFMS (Leco Corporation)
Ion Source Temperature	200 °C
Ionisation	EI at 70 eV
Mass Range	50-800 m/z
Acquisition rate	50 spectra/second
Detector Voltage	200 Voltage offset
Data Processing	ChromaTOF ver 4.72.0.0
Peak Finding	Non-Target Deconvolution
Peak Alignment	Statistical compare (Peak width 70)
Signal-to-noise	200, minimum of 3 apexing peaks
Library	NIST 20 (80% similarity threshold)

2.7. Data analysis

Raw data, including peak areas and annotations, acquired from serum and CSF samples using the Statistical Compare module of ChromaTOF, were exported to Microsoft Excel. Data from each sample matrix were processed and analysed independently. Compounds with identical names and unique masses (UMs) were combined to generate consolidated peak tables.

For data clean-up, potential contaminants were identified by using both system blanks and extraction blanks in line with Broadhurst et al. (2018). Peaks detected in the system blanks were excluded if their average concentration in study samples was ≤20-fold higher than in the blanks, while for the extraction blanks, peaks were removed if their average sample concentration was ≤3-fold greater than the blank. Peaks exceeding this ratio were retained and considered reliable signals. Data were normalised relative to the internal standard, and metabolite abundances expressed as relative concentrations (ng/µL).

To minimise systematic variation between analytical runs, batch effects were corrected by applying the EigenMS algorithm using MetaboAnalyst 6.0 (https://www.metaboanalyst.ca/, accessed February 2025). This method has been shown to effectively correct complex biases in high-dimensional datasets and was adapted here for use in metabolomics (Karpievitch et al., 2015).

Statistical analyses were performed in MetaboAnalyst 6.0, using these batch-corrected datasets. First, a 10% low-variance filter was applied based on the interquartile range (IQR). Missing values were then imputed using a limit-of-detection approach, replacing each missing entry with one-fifth of the minimum positive value for the corresponding compound across the dataset.

The datasets were log2-transformed to reduce heteroscedasticity and Pareto-scaled to balance the contribution of low- and high-abundance metabolites prior to statistical analyses.

Multivariate analyses were applied to evaluate overall variance structure and sample clustering, followed by univariate approaches to identify specific metabolites contributing to group differences. Unsupervised clustering was first explored using principal component analysis (PCA), followed by supervised discrimination using partial least squares–discriminant analysis (PLS-DA). In the PLS-DA model, compound contributions were visualised along component 1 and 2. Model validation was performed with a maximum of five components and 5-fold cross-validation, with predictive ability quantified by Q^2. Robustness of classification models was further assessed using permutation testing (2000 permutations) to calculate empirical p-values.

Univariate analyses included fold-change (FC), t-tests, and volcano plots. FC thresholds were set at FC ≥ 2.0 or FC ≤ 0.5, indicating up- or downregulation of compounds, respectively. Significance testing was further performed using unpaired, unequal variance, non-parametric t-tests. A raw $p < 0.05$ and false discovery rate (FDR)-adjusted $p < 0.05$ were considered statistically significant. To account for multiple testing and to identify statistically robust variations, metabolites were only considered significantly differential within each dataset if both the FC and the FDR-adjusted p-value thresholds between the positive and negative groups were met (FC ≥ 2.0 or FC ≤ 0.5 and FDR adjusted $p < 0.05$). Volcano plots were generated by combining FC and t-test results, using FC ≥ 2.0 or FC ≤ 0.5 and raw $p < 0.05$.

Pathway analysis was subsequently done on the list of annotated differential metabolites identified from the volcano plots for each sample matrix (serum and CSF) to explore the biological pathways potentially perturbed between groups. Only metabolites that could be matched to entries in the Human Metabolome Database (HMDB) and mapped to the Canis lupus familiaris (dog) KEGG pathway library were included. The analysis used the Global Test for pathway enrichment and relative betweenness centrality for topology assessment, with all compounds in the selected library (updated December 2024) serving as the reference metabolome. Results were visualised as scatter plots displaying significantly enriched pathways (FDR adjusted $p < 0.05$), where p-values from enrichment analysis were plotted against pathway impact scores.

The resulting list of statistically differential metabolites from each sample matrix was then subjected to receiver operating characteristic (ROC) curve analysis to evaluate their individual discriminatory performance in distinguishing between the positive and negative groups. Area under the curve (AUC) values were computed for each metabolite using the MetaboAnalyst classical univariate ROC curve analysis module. Group classification was defined according to rabies status, and optimal cut-off thresholds shown as closest to top-left corner.

3. Results

3.1. Cohort demographics

The signalment of both rabies-positive and rabies-negative dogs included in this study is shown in Table 1. All sampled dogs were of the Basenji breed. Age was classified as either puppy or adult because most owners could not provide accurate age information, and dentition-based age estimation was not feasible due to limited owner cooperation. Puppies were defined as dogs aged 6 months or below, while adult dogs were those older than 6 months.

Table 2: Demographic characteristics of rabies-positive and rabies-negative dogs included in this study,

Parameters	category	No Positive	No Negative	Total *n* (%)
Age	Puppy	3	2	5
	Adult	17	18	35
Sex	Female	8	8	16
	Male	12	12	24

3.2. GCxGC-TOFMS results

Chromatographic results of the FAMES standard over the analytical serum (supplementary Figure S1) and CSF batches (supplementary Figure S2) indicated acceptable instrument stability over the course of

the metabolomics analyses. Results of the system blanks and extraction blanks indicated minimal instrument and reagent contamination (supplementary Figure S3). Chromatograms of the analytical samples indicated some visual variations between the sample types as well as between positive and negative specimens (Figure 1).

3.3 Data overview

For the serum dataset, the initial raw data exported from ChromaTOF comprised 40 samples with 1344 compound peaks. After data clean-up, 965 compounds remained, of which 550 were annotated and 415 did not meet the minimum 80% library similarity threshold and were retained as unannotated analytes. Unannotated analytes were included in subsequent analyses to avoid excluding potentially biologically relevant, yet uncharacterised, variations. EigenMS batch-correction was applied (supplementary Figure S4). This corrected dataset contained 11.6% missing values (4494 entries) and after interquartile range (IQR) filtering, 97 low-variance compounds were removed, resulting in 868 compounds for analysis. Missingness was not significantly different between groups, either before (Kruskal-Wallis $p = 0.417$) or after filtering ($p = 0.409$).

For the CSF dataset, three samples (one negative and two positive) were excluded due to poor analytical quality, resulting in 37 samples with 694 compound peaks. After data clean-up, 334 compounds remained, of which 224 were annotated and 80 were retained as unannotated analytes. EigenMS batch-correction was applied for the CSF dataset (supplementary Figure S5). The corrected dataset contained 15.2% missing values (1879 entries). Following IQR filtering, 34 low-variance compounds were removed, resulting in 300 retained compounds. Missingness did not significantly differ between groups, either before ($p = 0.939$) or after filtering ($p = 0.903$).

PCA did not reveal clear separation between the positive and negative groups for either sample matrix (Figure 2). For the serum dataset, the first two principal components (PCs) explained a total of 30.9% of the variance (PC1 = 19.7%, PC2 = 11.2%), while for the CSF dataset, PC1 and PC2 accounted for 32.5% of the total variance (PC1 = 20.6%, PC2 = 11.9%). PLS-DA also didn't indicate separation, with cross-validation indicating limited predictive performance, the models were therefore not used for subsequent statistical analyses (supplementary Figures S6 and S7). The low degree of separation and explained variance may reflect high within-group biological variability, overlapping metabolic profiles between groups, or the asymptomatic status of the positive group at the time of sampling, suggesting only subtle metabolic alterations not detectable at the global level.

3.4 Differential metabolites

3.4.1. Serum metabolites analysis

In serum, the volcano plot analysis identified 60 differentially regulated compounds ($FC \geq 2.0$ or $FC \leq 0.5$, raw $p < 0.05$; Figure 3). Detailed results are provided in Supplementary Table S1.

Serum pathway analysis results are summarised in Supplementary Table S2, with significantly enriched pathways visualised in Figure 4.

The most significantly affected pathways included glycerolipid metabolism, glyoxylate and dicarboxylate metabolism, the pentose phosphate pathway, and glycine, serine, and threonine metabolism (Figure 3; Table S2, FDR $p < 0.05$). Among these pathways however, the only metabolite matched was glyceric acid, with threonine additionally identified in glycine, serine, and threonine metabolism. Furthermore, the pathway impact values were generally low, with glycerolipid metabolism showing the highest impact at 0.0934.

Following FDR correction, four serum metabolites (Analyte 634; Glyceric acid; Analyte 706 and Benzoic acid) remained statistically significant and were further evaluated for their discriminatory performance between the positive and negatives specimens, using ROC curve analysis (Detailed results in Table S3). All four compounds demonstrated strong classification potential between the study groups, with AUC values exceeding 0.848. The unannotated compound, Analyte 634 showed the highest discriminative ability (AUC = 0.962, 95% CI: 0.889–1.000), followed by glyceric acid (AUC = 0.925, 95% CI: 0.820–0.985), Analyte 706 (AUC = 0.854, 95% CI: 0.726–0.948), and benzoic acid (AUC = 0.848, 95% CI: 0.709–0.950). Box plots of these compounds are shown in Figure 5, with detailed AUC analysis results provided in the supplementary information, together with mass spectra for unannotated metabolites (Table S3 and Figure S8).

3.4.2. CSF metabolites analysis

In CSF volcano plot analysis revealed 6 differentially upregulated and 6 downregulated compounds ($FC \geq 2.0$ or $FC \leq 0.5$ and raw $p < 0.05$; Figure 6). Detailed results are provided in Supplementary Table S4.

Pathway analysis of the CSF differential data revealed several pathways with nominal enrichment (Figure 7; Supplementary Table S5). The most affected pathways included the pentose phosphate pathway (raw $p = 0.021$), glutathione metabolism (raw $p = 0.050$), and nicotinate and nicotinamide metabolism (raw $p = 0.070$). However, no pathways remained statistically significant after FDR correction (FDR > 0.05). Similar to the serum analysis, most pathway hits were driven by a single matched compound, although in CSF these compounds differed between the pathways.

After FDR correction, only one CSF compound (Analyte 369) remained statistically differential (Table S4). ROC analysis demonstrated strong discriminatory potential for Analyte 369, with an AUC of 0.924 (95% CI: 0.801–1.000). The box plot for Analyte 369 is shown in Figure 8, with detailed AUC analysis results and corresponding mass spectra provided in the Supplementary Information (Table S6 and Figure S9).

4. Discussion

In this study, we analyzed the metabolomic profiles of CSF and serum from Basenji dogs infected with rabies virus, but not yet exhibiting clinical signs. Our preliminary multivariate assessment of data

indicated no significant differences in both serum and CSF metabolites between the infected and control groups. This may be attributed to the fact that the infection was still in the incubation phase, during which the rabies virus evades host immunity and primarily targets neural tissue. At this early stage, most metabolic alterations in serum may therefore be subtle and not yet detectable.

However, when applying univariate analyses, a total of sixty (60) differentially regulated compounds were identified through volcano plot analysis. Pathway enrichment analysis showed that the most significantly affected pathways included glycerolipid metabolism, glyoxylate and dicarboxylate metabolism, the pentose phosphate pathway, and glycine, serine, and threonine metabolism, with glycerolipid metabolism exhibiting the highest impact. The glycerolipid pathway is responsible for the synthesis and degradation of glycerolipids, such as triglycerides, which play essential roles in energy storage, membrane structure, and cellular signaling (Klaus & Kohlwein, 2013, Zaremberg et al., 2019). Previous studies have demonstrated that rabies virus infection increases lipid droplet production and triglyceride synthesis in multiple cell types and in mouse brains (Zhao et al., 2022). This metabolic alteration is thought to facilitate rabies virus replication and budding by providing both structural support and a metabolic platform that enhances viral assembly. Viral matrix and glycoproteins, which are essential for virion assembly and budding, have been shown to associate with lipid droplets. These lipid droplets may serve as intracellular carriers that promote the trafficking of viral components to the cell membrane, thereby increasing viral production and release (Zhao et al., 2022). Consequently, the increased alteration of the glycerolipid pathway observed in this study likely reflects a viral strategy to optimize replication efficiency during the early stages of infection.

The second pathway identified in the pathway enrichment analysis of the sera was the glyoxylate and dicarboxylate pathway, which is involved in metabolic processes related to energy production. Although the glyoxylate pathway (or cycle) does not naturally operate in dogs or other vertebrates, it is a metabolic pathway found primarily in plants, bacteria, and fungi to convert fat into carbohydrates. Therefore, increased alteration in this pathway is not a typical disease mechanism in dogs. However, recent metabolomic studies have shown that dysregulation of pathways interacting with glyoxylate and dicarboxylate metabolism is associated with inflammatory disease states and organ dysfunction in dogs and other mammals, including geriatric trauma (Huang et al., 2025). Given the neurotropic nature of the rabies virus and its dependence on host metabolic processes for replication within neurons, disruption of this pathway, which regulates the conversion of glyoxylate to glycine or oxalate, may reflect altered neuronal energy metabolism during the early stages of infection. Similar perturbations of this pathway have been reported in canine babesiosis (Rubić et al., 2022), a highly inflammatory tick-borne disease, and in geriatric trauma, where they frequently co-occur with alterations in cysteine, methionine, glutathione, alanine, aspartate, and glutamate metabolism (Rubić et al., 2022). Together, these observations suggest that changes in glyoxylate and dicarboxylate metabolism may represent a common metabolic response to inflammation-associated neuronal stress, with potential relevance to rabies pathogenesis.

The pentose phosphate pathway was significantly altered in the serum pathway enrichment analysis. As a cytosolic pathway parallel to glycolysis, the pentose phosphate pathway generates NADPH and ribose-5-phosphate to support antioxidant defence, lipid and steroid biosynthesis, and nucleotide synthesis (Landau, 2013). Although its role in rabies virus infection remains poorly studied, a virus with similar neurological clinical manifestations, the pseudorabies virus, reprograms host metabolism to promote glycolysis and the pentose phosphate pathway, thereby enhancing nucleotide biosynthesis and viral replication (Gou et al., 2021). This highlights the pathway as a promising target for the development of antiviral interventions. Consequently, the increased pentose phosphate pathway metabolism observed in this study may result from similar metabolic reprogramming and warrants further investigation.

Among the three amino acid metabolic pathways significantly affected in this study; glycine, serine, and threonine metabolism, evidence suggests a critical role for serine in rabies virus (RABV) pathogenesis. Specifically, serine residues at positions S162 and S166 of the RABV phosphoprotein (P) are essential for its interaction with mitochondrial respiratory chain complex I, an interaction that initiates mitochondrial dysfunction (Kammouni et al., 2017) This dysfunction leads to oxidative stress in neurons, resulting in acute neurodegenerative changes and the severe neurological manifestations characteristic of rabies virus infection (Kammouni et al., 2017). These findings underscore the importance of serine metabolism in rabies virus infection and highlight its potential relevance in the development of novel therapeutic strategies against rabies.

Although there is limited information on the specific roles of altered glycine and threonine metabolism in rabies pathogenesis, the importance of amino acid metabolism in viral replication cannot be overemphasized. Rabies virus infection has been shown to induce differential ubiquitination of proteins involved in amino acid biosynthesis (Cai, et al., 2020). These proteins, particularly glycine, which functions as a neurotransmitter, are significantly enriched in the myelin sheath and in binding-related cellular functions, processes that are critical to the pathogenesis of rabies. (Cai, et al., 2020).

Four compounds demonstrated strong discriminatory potential between the positive and negative study groups: Analyte 634, glyceric acid, Analyte 706, and benzoic acid, with Analyte 634 exhibiting the highest discriminatory ability. Although Analytes 634 and 706 could not be identified using the available metabolic databases, their ability to clearly differentiate rabies-positive from rabies-negative serum samples suggests that they are important serum metabolites and warrant further investigation. Glyceric acid, on the other hand, is a key 3-carbon metabolic intermediate involved in glycolysis metabolism and plays a vital role in cellular energy regulation and as a precursor in organic synthesis (Hirvonen et al., 2021). A study of rabies infection in mice demonstrated increased glucose uptake in the brain during the late stage of infection with different rabies virus (RABV) strains, including the laboratory-attenuated CVS strain and the wild-type DRV strain (Pei et al., 2022). This enhanced glucose uptake may account for the elevated levels of glyceric acid observed in our study, considering that glyceric acid is a metabolic intermediate of glycolysis involved in energy production. Consequently, this metabolic alteration may underlie the observed separation of rabies virus infected samples from negative controls observed in this study.

Benzoic acid, identified as one of the discriminatory metabolites in the positive samples, can accumulate in dogs through dietary exposure, particularly from foods preserved with benzoic acid or sodium benzoate, as well as from certain dental products. Elevated intake may also occur when foods preserved with high levels of sodium benzoate are consumed alongside citric or ascorbic acid (Del Olmo et al., 2017). In dogs, benzoic acid is primarily metabolized via conjugation with glycine to form hippuric acid, which is subsequently excreted in the urine (Hutt & Caldwell, 1990). Although dogs can process and eliminate benzoic acid, it is considered a xenobiotic that is handled through detoxification pathways rather than being endogenously synthesized (Hutt & Caldwell, 1990). The accumulation of benzoic acid observed in the positive serum samples, to an extent that allows it to serve as a differentiating metabolite, may therefore reflect rabies virus-induced alterations in the glycine conjugation pathway, leading to impaired clearance and serum accumulation. Further investigation of benzoic acid conjugation and detoxification pathways in rabies-infected dogs is warranted to elucidate the underlying mechanism.

In addition to the pentose phosphate pathway, which was the most affected pathway in the CSF pathway analysis, differential analysis revealed two other pathways with nominal enrichment: glutathione metabolism and nicotinate and nicotinamide metabolism. Glutathione is a key intracellular antioxidant that neutralizes free radicals and reactive oxygen species, thereby preventing oxidative stress and cellular damage. In addition to its antioxidant function, glutathione plays essential roles in detoxification, immune support, maintenance of cellular functions, and tissue repair (Hayes & McLellan, 1999; Averill-Bates, 2023). Alterations in glutathione homeostasis and glutathione-dependent enzyme activities are key contributors to the initiation and progression of several neurodegenerative diseases, including Alzheimer’s disease, Parkinson’s disease, Huntington’s disease, amyotrophic lateral sclerosis, and Friedreich’s ataxia (Johnson et al., 2012). Rabies virus infection has been shown to induce mitochondrial dysfunction, leading to oxidative stress, overproduction of reactive oxygen species, and degenerative neuronal changes, such as axonal swelling, lipid peroxidation, and reduced axonal growth (Jackson et al., 2011 Alandijany et al., 2013). Therefore, the increased glutathione metabolism observed in this study may reflect a compensatory cellular response aimed at counteracting rabies virus-induced oxidative stress.

Nicotinate and nicotinamide metabolism was also identified as a differentially enriched pathway in the CSF pathway analysis. Previous studies have demonstrated that nicotinic acetylcholine receptors at the neuromuscular junction, located at the site of rabies virus inoculation following a rabid dog bite, represent the first identified receptors and molecular targets of the virus (Guo et al., 2019; Lian et al., 2022). The rabies virus glycoprotein, which is the sole external protein on the virion surface, plays a critical role in mediating viral attachment and entry into host cells and serves as the primary target for neutralizing antibodies (Yang et al., 2020). The interaction between the rabies virus glycoprotein and host nicotinic acetylcholine receptors facilitates viral entry and influences host immune responses (O'Brien, et al., 2024). The identification of alterations in nicotinate and nicotinamide metabolism in the CSF may therefore reflect metabolic perturbations associated with rabies virus-host receptor interactions during infection.

Indolelactic acid was identified in both the serum and CSF datasets during volcano plot analysis based on fold-change and raw *p*-value thresholds, and was found to be consistently downregulated in the positive group. Indole-derived metabolites, which originate from microbial tryptophan metabolism, are known to function as signaling molecules that influence gut-brain axis communication, immune regulation, and metabolic homeostasis (Chen et al., 2022; Shaheen et al., 2025). Altered levels of these metabolites have previously been reported in the CSF and urine of individuals with neuropsychiatric disorders, suggesting a role in central nervous system function. Experimental evidence further indicates that indolelactic acid exerts neuroprotective effects, as prolonged administration has been shown to ameliorate depression- and anxiety-like behaviors, restore hypothalamic-pituitary-adrenal axis function, enhance brain-derived neurotrophic factor expression, and modulate serotonin signaling in animal models (Chen et al., 2022). Although direct evidence linking indolelactic acid to rabies virus infection is currently lacking, the consistent downregulation of this metabolite in both CSF and serum observed in the present study may be indicative of disrupted neuroprotective and immunomodulatory pathways. Given the capacity of the rabies virus to induce neuroinflammation and oxidative stress, reduced levels of indole-related metabolites may exacerbate neuronal vulnerability and contribute to disease pathogenesis. Further studies are warranted to clarify the mechanistic role of indolelactic acid and related metabolites in rabies-associated neuronal dysfunction.

Furthermore, the unique mass, retention time, and mass spectra of the significant compounds, Serum Analyte 634 and CSF Analyte 369 (refer to Appendix I, Tables S3 and S6 of supplementary information), closely matched, suggesting that they likely represent the same compound. These peaks were detected at very low concentrations in the negative groups and at even lower levels in the positive groups. This observation and the putative compound identification warrant further investigation in future studies.

4.2. Conclusion

This study provides novel insight into early metabolic alterations associated with rabies virus infection in Basenji dogs during the incubation phase, prior to the onset of clinical signs. While metabolic profiles may be affected by variables such as breed, nutrition, health status, and overall wellbeing, and despite minimal multivariate differences between infected and control groups, differential and pathway-based analyses revealed distinct metabolic perturbations in both serum and CSF. Key pathways affected included glycerolipid metabolism, glyoxylate and dicarboxylate metabolism, the pentose phosphate pathway, amino acid metabolism (glycine, serine, and threonine), glutathione metabolism, and nicotinate and nicotinamide metabolism, highlighting early disruptions in energy production, lipid utilization, redox balance, and neuronal metabolic homeostasis. Several metabolites, including glyceric acid, benzoic acid, and two unidentified analytes, demonstrated strong discriminatory potential between rabies-positive and negative samples, underscoring their promise as candidate biomarkers. The identification of annotated discriminatory metabolites warrants the need for future, more elaborative studies. Collectively, these findings suggest that the rabies virus induces subtle but biologically meaningful metabolic reprogramming during the preclinical stage of infection, likely reflecting viral strategies to support replication and modulate host neuronal and immune responses. Further targeted and longitudinal

studies are warranted to validate these metabolites and pathways and to elucidate their mechanistic roles in rabies pathogenesis and early diagnosis.

4.3. Limitation

The cross-sectional design of this study, together with the absence of longitudinal sampling, limited the ability to assess temporal metabolic changes during disease progression. Longitudinal follow-up was not feasible, as all sampled dogs were subsequently slaughtered for human consumption, precluding repeated sampling over time.

Declarations

Data availability statement

The original contributions presented in the study are included in the article/supplementary material. Further inquiries can be directed to the corresponding authors.

Ethics statement

All protocols for this study were reviewed and approved on the 28th of March, 2023 by the Institutional Animal Care and Use Committee (IACUC) of the Faculty of Veterinary Medicine, University of Nigeria, Nsukka (Approval No: FVM-UNN-IACUC-2023-03100) before the commencement of the research. Additionally, the ethical approval for the use of animals in research was granted on the 28th of March, 2023 by the South African National Animal Ethics Committee in accordance with Section 20 of the Animal Diseases Act of 1984 (Act No. 35 of 1984), reference number 12/11/1/1/8 (6640KL).

Authors contributions:

Conceptualization, U.U.E and C.T.S; Data curation, U.U.E, K.I.O, E.C.N, M.M HLE; Formal analysis, M.O, I.D, E.D.; Funding acquisition, U.U.E and C.T.S; Investigation, U.U.E., E.C.N., M.M., B.M.A., R.C.E., HLE C.T.S; Methodology, U.U.E., K.I.O, I.D, H.L.E, C.T.S, M.O, I.D, E.D.; Project administration, C.T.S; Resources, U.U.E., C.T.S; Supervision, R.C.E., B.M.A., C.T.S; Validation, U.U.E., M.O, I.D, C.T.S; Visualization, U.U.E., M.O, E.D. I.D, C.T.S; Writing—original draft, U.U.E. M.O, E.D, Writing—review and editing, U.U.E., M.O., E.D., K.I.O., E.C.N., M.M. R.C.E., B.M.A., HLE., I.D., C.T.S.

Funding:

Africa Research Excellence FundResearch Development Fellowships 2022/23 (AREF-312-EZE-F-C0953).

Conflicts of Interest:

The authors declare no conflicts of interest.

Generative AI statement

The author(s) declared that generative AI was not used in the creation of this manuscript.

Acknowledgments:

The authors gratefully acknowledge the Africa Research Excellence Fund for funding this research. We also thank the Agricultural Research Council – Onderstepoort Veterinary Research, Rabies Laboratory and Transboundary Animal Diseases, South Africa; Centre for Human Metabolomics, Desmond Tutu School of Medicine, Faculty of Health Sciences, North-West University, Potchefstroom, South Africa and the Rabies Unit, National Veterinary Research Institute, Vom, Nigeria, for their structural support in conducting the laboratory analyses. We further appreciate the University of Nigeria and the University of Pretoria for providing an enabling environment that facilitated this research.

References

1. Abubakar, A. T., Al-Mustapha, A. I., Oyewo, M., Ibrahim, A., Abdulrahim, I., Yakub, J. M., Elelu, N., Nguku, P., Balogun, M. S., Awosanya, E. J., Kia, G. S. N., Kwaga, J. K. P., Okoli, I., Bolajoko, M. B., Alimi, Y., Mbilo, C., & Dacheux, L. (2024). 'Prospects for dog rabies elimination in Nigeria by 2030', *Zoonoses and Public Health*, 71(1), pp. 1–17. Available at: https://doi.org/10.1111/zph.13084
2. Akanbi, I. O., Ishola, O. O., Olugasa, B. O., Akanbi, I. M., & Olarinmoye, A. O. (2023). 'Rabies exposure and prophylaxis among dog owners in Ogun State, Nigeria: a descriptive and categorical analysis of knowledge, attitudes and practices', *One Health Implementation Research*, 3, pp. 135–147. Available at: http://dx.doi.org/10.20517/ohir.2023.29
3. Alandijany, T., Kammouni, W., Chowdhury, R., Fernyhough, S. K., P. and, & Jackson, A. C. (2013). 'Mitochondrial dysfunction in rabies virus infection of neurons', *Journal of NeuroVirology*, 19(6), pp. 537–549. Available at: https://doi.org/10.1007/s13365-013-0214-6
4. Atuman, Y. J., Adawa, D. A. Y., Audu, S. W., Mshelbwala, P. P., & Ogunkoya, A. B. (2014). Potential risks for rabies spill-over from apparently healthy dogs to wildlife in Bauchi State, Nigeria. *Journal of Veterinary Advances*, *4*, 493–498.
5. Averill-Bates, D. A. (2023). 'The antioxidant glutathione', *Vitamins and Hormones*, 121, pp. 109–141. Available at: https://doi.org/10.1016/bs.vh.2022.09.002
6. Blasco, H., Corcia, P., Moreau, C., Veau, S., Fournier, C., Vourc'h, P., Emond, P., Gordon, P., Pradat, P. F., Praline, J., Devos, D., Nadal-Desbarats, L., & Andres, C. R. (2010). '^{1}H-NMR-based metabolomic profiling of CSF in early amyotrophic lateral sclerosis', *PLoS ONE*, 5(10), e13223. Available at: https://doi.org/10.1371/journal.pone.0013223
7. Cai, Y., Su, J., Wang, N., Zhao, W., Zhu, M., & Su, S. (2020). 'Comprehensive analysis of the ubiquitome in rabies virus-infected brain tissue of *Mus musculus*', *Veterinary Microbiology*, 241, 108552. Available at: https://doi.org/10.1016/j.vetmic.2019.108552
8. Chen, Y., Tian, P., Wang, Z., Pan, R., Shang, K., Wang, G., Zhao, J., & Chen, W. (2022). 'Indole acetic acid exerts anti-depressive effects on an animal model of chronic mild stress', *Nutrients*, 14(23), 5019. Available at: https://doi.org/10.3390/nu14235019

9. Coen, M., O'Sullivan, M., Bubb, W. A., Kuchel, P. W., & Sorrell, T. (2005). 'Proton nuclear magnetic resonance-based metabonomics for rapid diagnosis of meningitis and ventriculitis', *Clinical Infectious Diseases*, 41(11), pp. 1582–1590. Available at: https://doi.org/10.1086/497836
10. Conceição, P., & Abreu, C. (2021). 'Raiva humana: optimização da prevenção e caminhos para a cura [Human rabies: optimization of prevention and paths towards the cure]', *Acta Médica Portuguesa*, 34(11), pp. 767–773. Available at: https://doi.org/10.20344/amp.10657
11. Dean, D. J., Abelseth, M. K., & Atanasiu, P. (1996). The fluorescent antibody test. In F. X. Meslin, M. M. Kaplan, & H. Koprowski (Eds.), *Laboratory Techniques in Rabies* (4th ed., pp. 88–95). World Health Organization.
12. Del Olmo, A., Calzada, J., & Nuñez, M. (2017). 'Benzoic acid and its derivatives as naturally occurring compounds in foods and as additives: uses, exposure, and controversy', *Critical Reviews in Food Science and Nutrition*, 57(14), pp. 3084–3103. Available at: https://doi.org/10.1080/10408398.2015.1087964
13. Eugene, E. C., Odunze, P., Nuhu, B., Olugbade, O. T., Dauda, M., Egwuenu, A., Samuel, O. W., & Okagbue, A. I. (2025). 'Rabies knowledge and prevention practices in Gombe State, Nigeria: a community-based comparative cross-sectional study of rabies hotspot and non-hotspot areas', *BMC Public Health*, 25, p. 177. Available at: https://doi.org/10.1186/s12889-025-21309-2
14. Eze, U. U., Coetzer, A., Scott, T. P., Anene, B. M., Ezeokonkwo, R. C., Nwosuh, C. I., Nel, L. H., & Sabeta, C. T. (2020). 'Economic and feasibility comparison of the dRIT and DFA for decentralized rabies diagnosis in resource-limited settings: the use of Nigerian dog meat markets as a case study', *PLoS Neglected Tropical Diseases*, 14(2), e0008088. Available at: https://doi.org/10.1371/journal.pntd.0008088
15. Eze, U. U., Ngoepe, E. C., Anene, B. M., Ezeokonkwo, R. C., Nwosuh, C., & Sabeta, C. T. (2018). 'Detection of Lyssavirus antigen and antibody levels among apparently healthy and suspected rabid dogs in South-Eastern Nigeria', *BMC Research Notes*, 11(1), p. 920. Available at: https://doi.org/10.1186/s13104-018-4024-z
16. Fooks, A., & Jackson, A. (2020). *Rabies: Scientific Basis of the Disease and its Management* (4th ed.). Elsevier.
17. Gou, H., Bian, Z., Li, Y., Cai, R., Jiang, Z., Song, S., Zhang, K., Chu, P., Yang, D., & Li, C. (2021). 'Metabolomics exploration of pseudorabies virus reprogramming metabolic profiles of PK-15 cells to enhance viral replication', *Frontiers in Cellular and Infection Microbiology*, 10, 599087. Available at: https://doi.org/10.3389/fcimb.2020.599087
18. Guo, Y., Duan, M., Wang, X., Gao, J., Guan, Z., & Zhang, M. (2019). 'Early events in rabies virus infection: attachment, entry, and intracellular trafficking', *Virus Research*, 263, pp. 217–225. Available at: https://doi.org/10.1016/j.virusres.2019.02.006
19. Hampson, K., Coudeville, L., Lembo, T., Sambo, M., Kieffer, A., Attlan, M., Barrat, J., Blanton, J. D., Briggs, D. J., Cleaveland, S., Costa, P., Freuling, C. M., Hiby, E., Knopf, L., Leanes, F., Meslin, F. X., Metlin, A., Miranda, M. E., Müller, T., & Nel, L. H. (2015). and Global Alliance for Rabies Control

Partners for Rabies Prevention 'Estimating the global burden of endemic canine rabies', *PLoS Neglected Tropical Diseases*, 9(4), e0003709. Available at: https://doi.org/10.1371/journal.pntd.0003709

20. Hartonen, M., Mattila, I., Ruskeepää, A. L., Orešič, M., & Hyötyläinen, T. (2013). 'Characterization of cerebrospinal fluid by comprehensive two-dimensional gas chromatography coupled to time-of-flight mass spectrometry', *Journal of Chromatography A*, 1293, pp. 142–149. Available at: https://doi.org/10.1016/j.chroma.2013.04.005
21. Hayes, J. D., & McLellan, L. I. (1999). 'Glutathione and glutathione-dependent enzymes represent a co-ordinately regulated defence against oxidative stress', *Free Radical Research*, 31(4), pp. 273–300. Available at: https://doi.org/10.1080/10715769900300851
22. Hirvonen, O. P., Kyröläinen, H., Lehti, M., & Kainulainen, H. (2021). 'Randomized trial: D-glyceric acid activates mitochondrial metabolism in 50–60-year-old healthy humans', *Frontiers in Aging*, 2, 752636. Available at: https://doi.org/10.3389/fragi.2021.752636
23. Huang, C., Gou, Y., Cong, Y., Li, D., Yang, J., & Feng, K. (2025). 'Metabolomics reveals glyoxylate and dicarboxylate metabolism disorder in elderly trauma: a retrospective study', *Clinical Interventions in Aging*, 20, pp. 2049–2064. Available at: https://doi.org/10.2147/CIA.S552626
24. Hutt, A. J., & Caldwell, J. (1990). Amino acid conjugation. In G. J. Mulder (Ed.), *Conjugation Reactions in Drug Metabolism: An Integral Approach* (pp. 273–300). Taylor & Francis Ltd.
25. International Committee on Taxonomy of Viruses (ICTV) (2025). *Virus taxonomy: classification and nomenclature of viruses: online report of the International Committee on Taxonomy of Viruses*. Available at: https://ictv.global/report (Accessed: 2025).
26. Jackson, A. C., Kammouni, W., & Fernyhough, P. (2011). 'Role of oxidative stress in rabies virus infection', *Advances in Virus Research*, 79, pp. 127–138. Available at: https://doi.org/10.1016/B978-0-12-387040-7.00008-1
27. Johnson, W. M., Wilson-Delfosse, A. L., & Mieyal, J. J. (2012). 'Dysregulation of glutathione homeostasis in neurodegenerative diseases', *Nutrients*, 4(10), pp. 1399–1440. Available at: https://doi.org/10.3390/nu4101399
28. Kammouni, W., Wood, H., & Jackson, A. C. (2017). 'Serine residues at positions 162 and 166 of the rabies virus phosphoprotein are critical for the induction of oxidative stress in rabies virus infection', *Journal of Neurovirology*, 23(3), pp. 358–368. Available at: https://doi.org/10.1007/s13365-016-0506-8
29. Karpievitch, Y. V., Nikolic, S. B., Wilson, R., Sharman, J. E., & Edwards, L. M. (2014). 'Metabolomics data normalization with EigenMS', *PLOS ONE*, 9, e116221. Available at: https://doi.org/10.1371/journal.pone.0116221
30. Klaus, N., & Kohlwein, S. D. (2013). Yeast and cancer cells – common principles in lipid metabolism. *Biochimica et Biophysica Acta (BBA) – Molecular and Cell Biology of Lipids*, *1831*(2), 314–326.
31. Lamas, C. C., Martinez, A. J., Baraff, R., & Bajwa, J. (1980). 'Rabies encephaloradiculomyelitis', *Acta Neuropathologica*, 51(3), pp. 245–247. Available at: https://doi.org/10.1007/BF00687393

32. Landau, B. R. (2013). 'Pentose phosphate (hexose monophosphate) pathway', in Lennarz, W.J. and Lane, M.D. (Eds.) *Encyclopedia of Biological Chemistry*. 2nd edn. Academic Press, pp. 391–395. Available at: https://doi.org/10.1016/B978-0-12-378630-2.00028-1
33. Lian, M., Hueffer, K., & Weltzin, M. M. (2022). 'Interactions between the rabies virus and nicotinic acetylcholine receptors: a potential role in rabies virus induced behavior modifications', *Heliyon*, 8(9), e10434. Available at: https://doi.org/10.1016/j.heliyon.2022.e10434
34. Mshelbwala, P. P., Weese, J. S., Sanni-Adeniyi, O. A., Chakma, S., Okeme, S. S., Mamun, A. A., Rupprecht, C. E., & Magalhaes, R. J. S. (2021). 'Rabies epidemiology, prevention and control in Nigeria: scoping progress towards elimination', *PLoS Neglected Tropical Diseases*, 15(8), e0009617. Available at: https://doi.org/10.1371/journal.pntd.0009617
35. Muñoz-Prieto, A., González-Arostegui, L. G., Rubić, I., Cerón, J. J., Tvarijonaviciute, A., Horvatić, A., & Mrljak, V. (2021). 'Untargeted metabolomic profiling of serum in dogs with hypothyroidism', *Research in Veterinary Science*, 136, pp. 6–10. Available at: https://doi.org/10.1016/j.rvsc.2021.01.023
36. O'Brien, B. C. V., Thao, S., Weber, L., Danielson, H. L., Boldt, A. D., Hueffer, K., & Weltzin, M. M. (2024). 'The human alpha7 nicotinic acetylcholine receptor is a host target for the rabies virus glycoprotein', *Frontiers in Cellular and Infection Microbiology*, 14, 1394713. Available at: https://doi.org/10.3389/fcimb.2024.1394713
37. Pei, J., Yuan, Y., Tian, D., Huang, F., Zhang, C., Wang, C., Zhou, M., Chen, H., Fu, Z., & Zhao, L. (2022). 'Comprehensive analysis of protein acetylation and glucose metabolism in mouse brains infected with rabies virus', *Journal of Virology*, 96, e01942-21. Available at: https://doi.org/10.1128/jvi.01942-21
38. Qiu, S., Cai, Y., Yao, H., Lin, C., Xie, Y., Tang, S., & Zhang, A. (2023). 'Small molecule metabolites: discovery of biomarkers and therapeutic targets', *Signal Transduction and Targeted Therapy*, 8(1), p. 132. Available at: https://doi.org/10.1038/s41392-023-01399-3
39. Rubić, I., Burchmore, R., Weidt, S., Regnault, C., Kuleš, J., Barić Rafaj, R., Mašek, T., Horvatić, A., Crnogaj, M., Eckersall, P. D., Novak, P., & Mrljak, V. (2022). 'Multi-platform strategies and metabolomics approaches for the investigation of comprehensive metabolite profile in dogs with *Babesia canis* infection', *International Journal of Molecular Sciences*, 23(3), p. 1575. Available at: https://doi.org/10.3390/ijms23031575
40. Rupprecht, C. E. (1996). 'Rhabdoviruses: rabies virus', in Baron, S. (Ed.) *Medical Microbiology*. 4th edn. Galveston (TX): University of Texas Medical Branch at Galveston. Available at: https://www.ncbi.nlm.nih.gov/books/NBK8618/
41. Shaheen, N., Miao, J., Xia, B., Zhao, Y., & Zhao, J. (2025). 'Multifaceted role of microbiota-derived indole-3-acetic acid in human diseases and its potential clinical application', *FASEB Journal*, 39(11), e70574. Available at: https://doi.org/10.1096/fj.202500295R
42. Sinclair, A., Viant, M., Ball, A., Burdon, M., Walker, E., Stewart, P., Rauz, S., & Young, S. (2010). 'NMR-based metabolomic analysis of cerebrospinal fluid and serum in neurological diseases – a

diagnostic tool?', *NMR in Biomedicine*, 23(2), pp. 123–132. Available at: https://doi.org/10.1002/nbm.1428

43. Swanepoel, A. C., Bester, J., Emmerson, O., Soma, P., Beukes, D., van Reenen, M., Loots, D. T., & du Preez, I. (2020). 'Serum metabolome changes in relation to prothrombotic state induced by combined oral contraceptives with drospirenone and ethinylestradiol', *OMICS: A Journal of Integrative Biology*, 24(7), pp. 404–414. Available at: https://doi.org/10.1089/omi.2020.0009
44. Thrusfield, M. (2005). *Veterinary Epidemiology* (3rd ed., pp. 233–234). Blackwell Science.
45. Tounta, V., Liu, Y., Cheyne, A., & Larrouy-Maumus, G. (2021). 'Metabolomics in infectious diseases and drug discovery', *Molecular Omics*, 17(3), pp. 376–393. Available at: https://doi.org/10.1039/d1mo00017a
46. Walker, H. K., Boag, A. M., Ottka, C., Lohi, H., Handel, I., Gow, A. G., & Mellanby, R. J. (2022). 'Serum metabolomic profiles in dogs with chronic enteropathy', *Journal of Veterinary Internal Medicine*, 36(5), pp. 1752–1759. Available at: https://doi.org/10.1111/jvim.16419
47. Warrell, D. A., Davidson, N. M., Pope, H. M., Bailie, W. E., Lawrie, J. H., Ormerod, L. D., Kertesz, A., & Lewis, P. (1976). 'Pathophysiologic studies in human rabies', *American Journal of Medicine*, 60(2), pp. 180–190. Available at: https://doi.org/10.1016/0002-9343(76)90427-7
48. Willoughby, R. E., Opladen, T., Maier, T., Rhead, W., Schmiedel, S., Hoyer, J., Drosten, C., Rupprecht, C., Hyland, K., & Hoffmann, G. (2009). 'Tetrahydrobiopterin deficiency in human rabies', *Journal of Inherited Metabolic Disease*, 32(1), pp. 65–72. Available at: https://doi.org/10.1007/s10545-008-0949-z
49. Willoughby, R. E., Roy-Burman, A., Martin, K. W., Christensen, J. C., Westenkirschner, D. F., Fleck, J. D., Glaser, C., Hyland, K., & Rupprecht, C. E. (2008). 'Generalised cranial artery spasm in human rabies', *Developments in Biologicals (Basel)*, 131, pp. 367–375.
50. World Health Organization. (2018). *Zero by 30: The global strategic plan to end human deaths from dog-mediated rabies by 2030*. WHO.
51. World Health Organization (2024). 'Rabies'. Available at: https://www.who.int/news-room/fact-sheets/detail/rabies (Accessed: 25 June 2025).
52. Yang, F., Lin, S., Ye, F., Yang, J., Qi, J., Chen, Z., Lin, X., Wang, J., Yue, D., Cheng, Y., Chen, Z., Chen, H., You, Y., Zhang, Z., Yang, Y., Yang, M., Sun, H., Li, Y., Cao, Y., Yang, S., Wei, Y., Gao, G. F., & Lu, G. (2020). 'Structural analysis of rabies virus glycoprotein reveals pH-dependent conformational changes and interactions with a neutralizing antibody', *Cell Host & Microbe*, 27(3), pp. 441–453.e7. Available at: https://doi.org/10.1016/j.chom.2019.12.012
53. Zaremberg, V., Ganesan, S., & Shabits, B. N. (2019). 'Metabolism and regulation of glycerolipids in yeast', in Geiger, O. (Ed.) *Biogenesis of Fatty Acids, Lipids and Membranes*. Handbook of Hydrocarbon and Lipid Microbiology. Cham: Springer. Available at: https://doi.org/10.1007/978-3-319-50430-8_20
54. Zhao, J., Zeng, Z., Chen, Y., Liu, W., Chen, H., Fu, Z. F., Zhao, L., & Zhou, M. (2022). 'Lipid droplets are beneficial for rabies virus replication by facilitating viral budding', *Journal of Virology*, 96(2), e01473-

21. Available at: https://doi.org/10.1128/JVI.01473-21

55. Zhao, P., Hou, K., Yang, S., & Xia, X. (2020). 'Characterization of small metabolites alteration in mice brain tissues after infection by rabies virus', *Infection, Genetics and Evolution*, 85, 104571. Available at: https://doi.org/10.1016/j.meegid.2020.104571

56. Zheng, W. B., Zou, Y., Elsheikha, H. M. (2019). 'Serum metabolomic alterations in Beagle dogs experimentally infected with *Toxocara canis*', *Parasites & Vectors*, 12, p. 447. Available at: https://doi.org/10.1186/s13071-019-3703-5

Figures

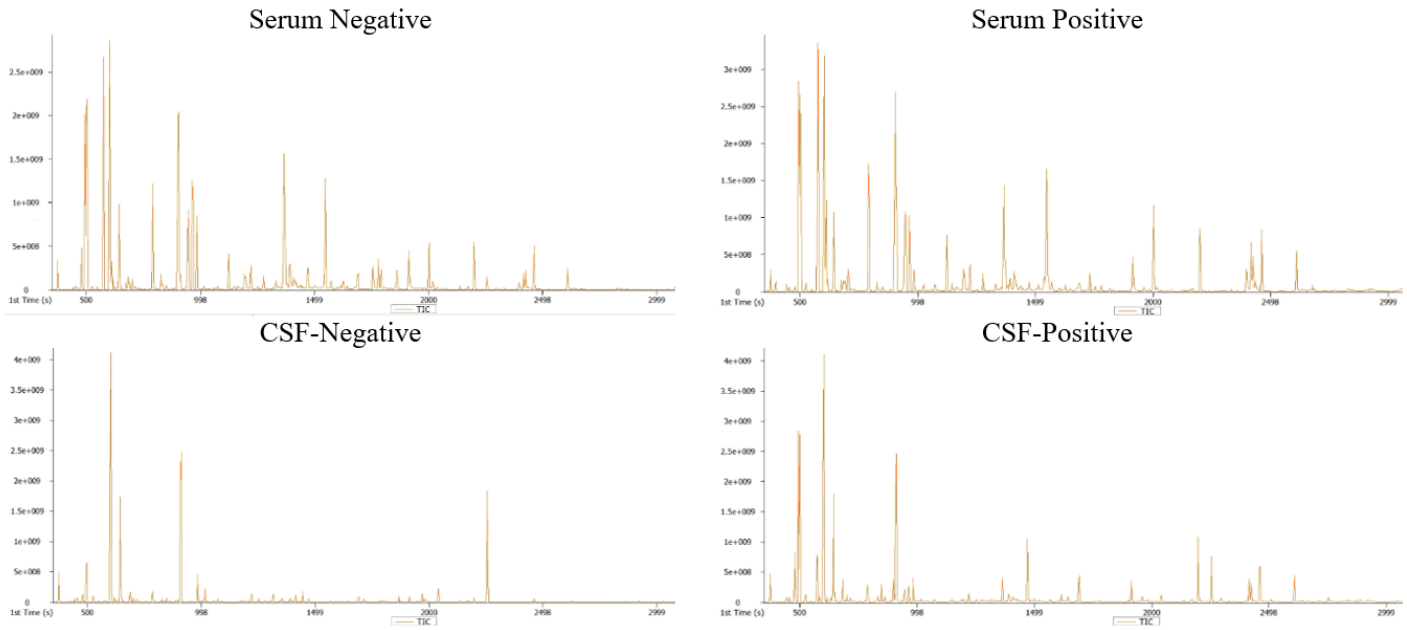


Figure 1

The chromatograms generated for both positive and negative serum specimens (top) as well as positive and negative CSF specimens (bottom).

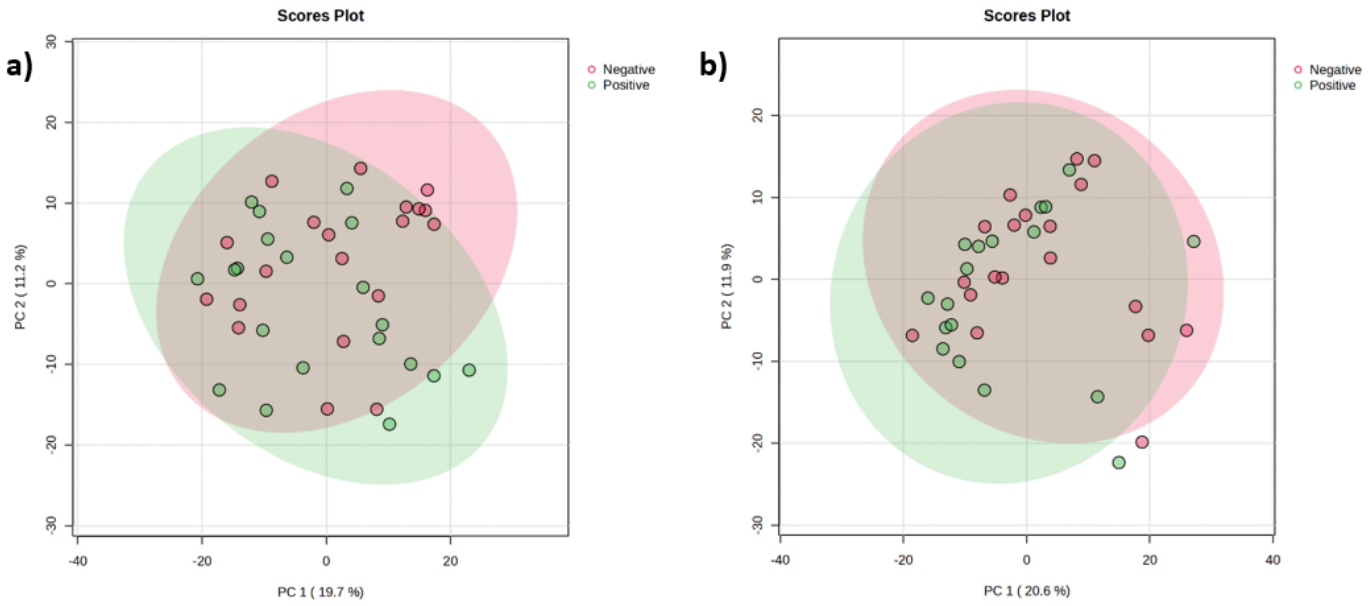


Figure 2

Principal component analysis (PCA) of the (a) serum and (b) CSF metabolite datasets demonstrating clustering by positive and negative study groups.

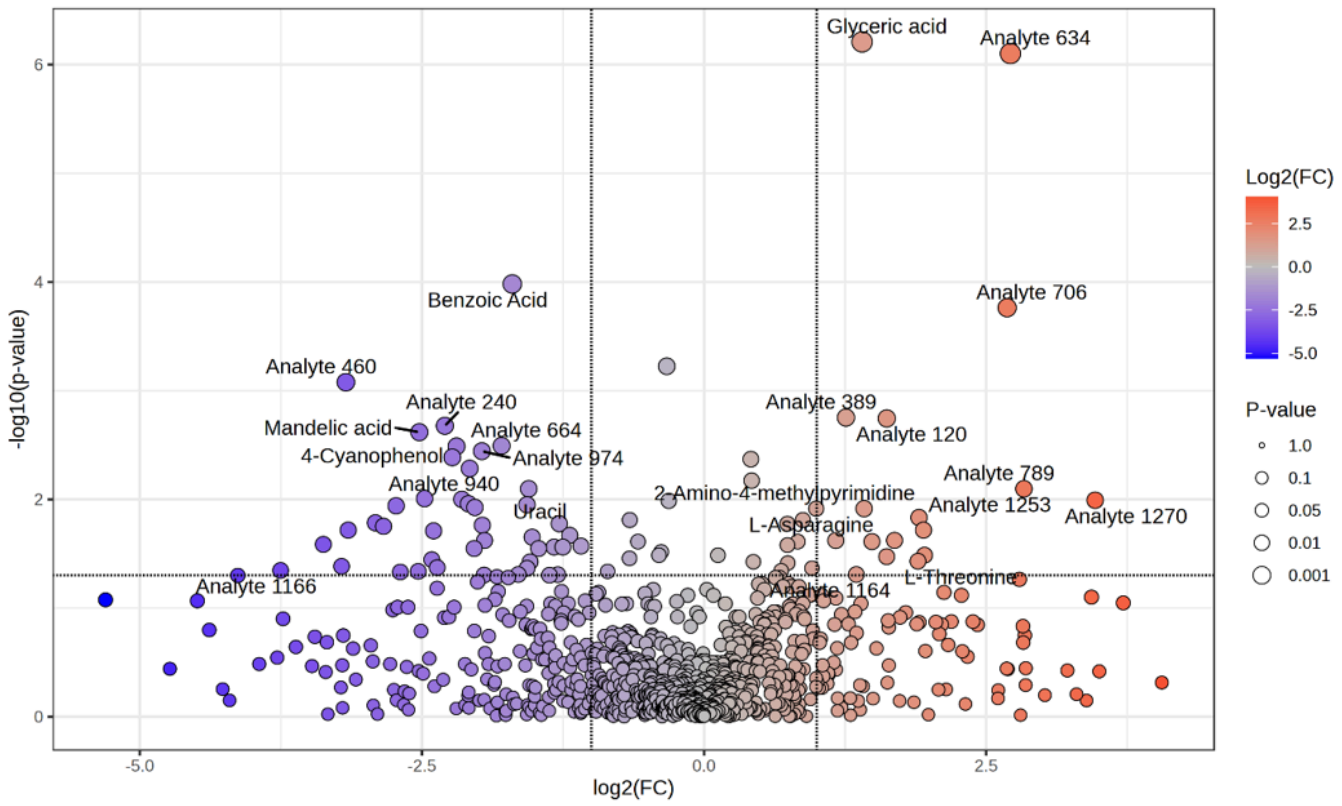


Figure 3

Volcano plot displaying the distribution of serum metabolites according to their log_2 fold change (x-axis) and -log_{10}(p-value) (y-axis). Metabolites with a raw p < 0.05 and FC ≥ 2.0 or FC ≤ 0.5 are indicated, representing those significantly altered between positive and negative specimens. Analytes represent unannotated compounds.

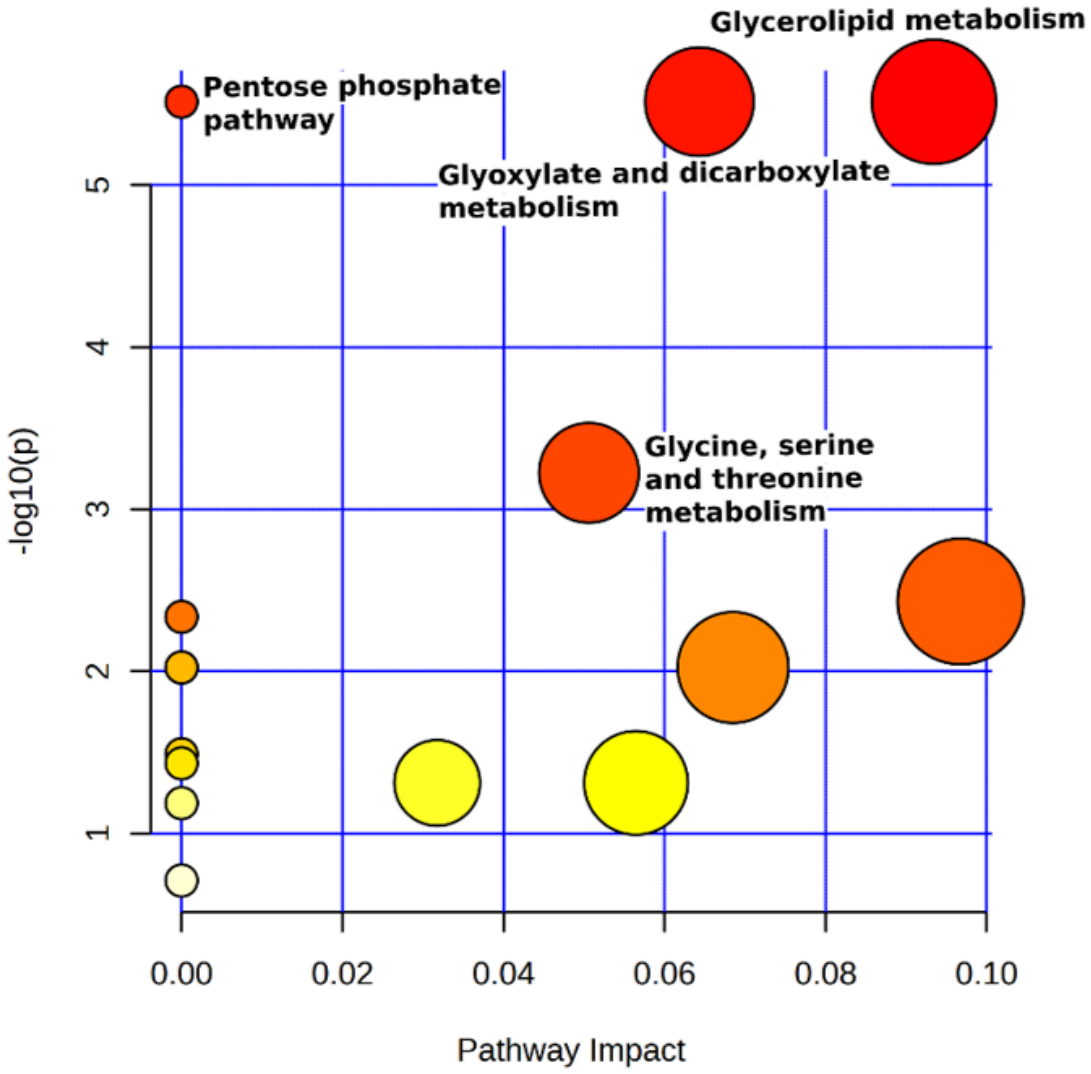


Figure 4

Pathway analysis of serum metabolites identified from initial differential metabolite analysis. Pathways are ranked according to pathway impact (x-axis) and $-log_{10}$(p-value) (y-axis), reflecting both the magnitude of metabolite enrichment and statistical significance. Larger and darker nodes indicate pathways with greater impact and significance. Annotated pathways represent those most affected between positive and negative study groups.

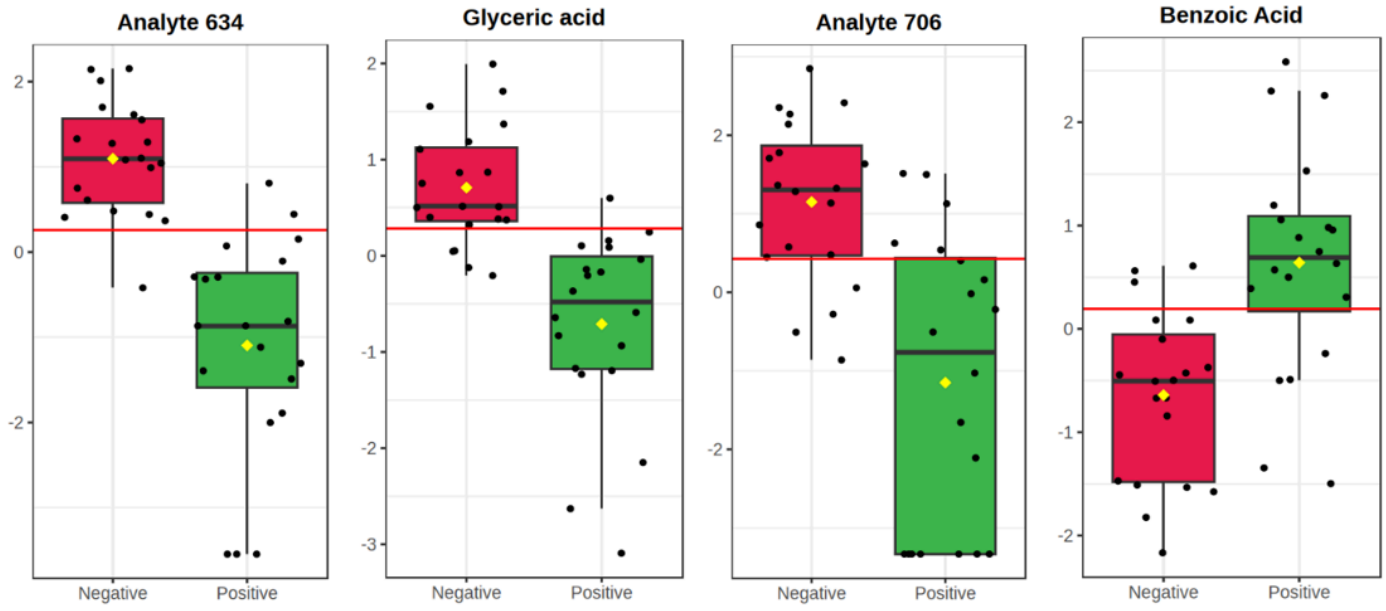


Figure 5

Box plot of serum differential metabolites from ROC analysis. The red horizontal line denotes the optimal classification cutoff determined by the ROC model, representing the threshold value that best separates the two groups based on metabolite intensity.

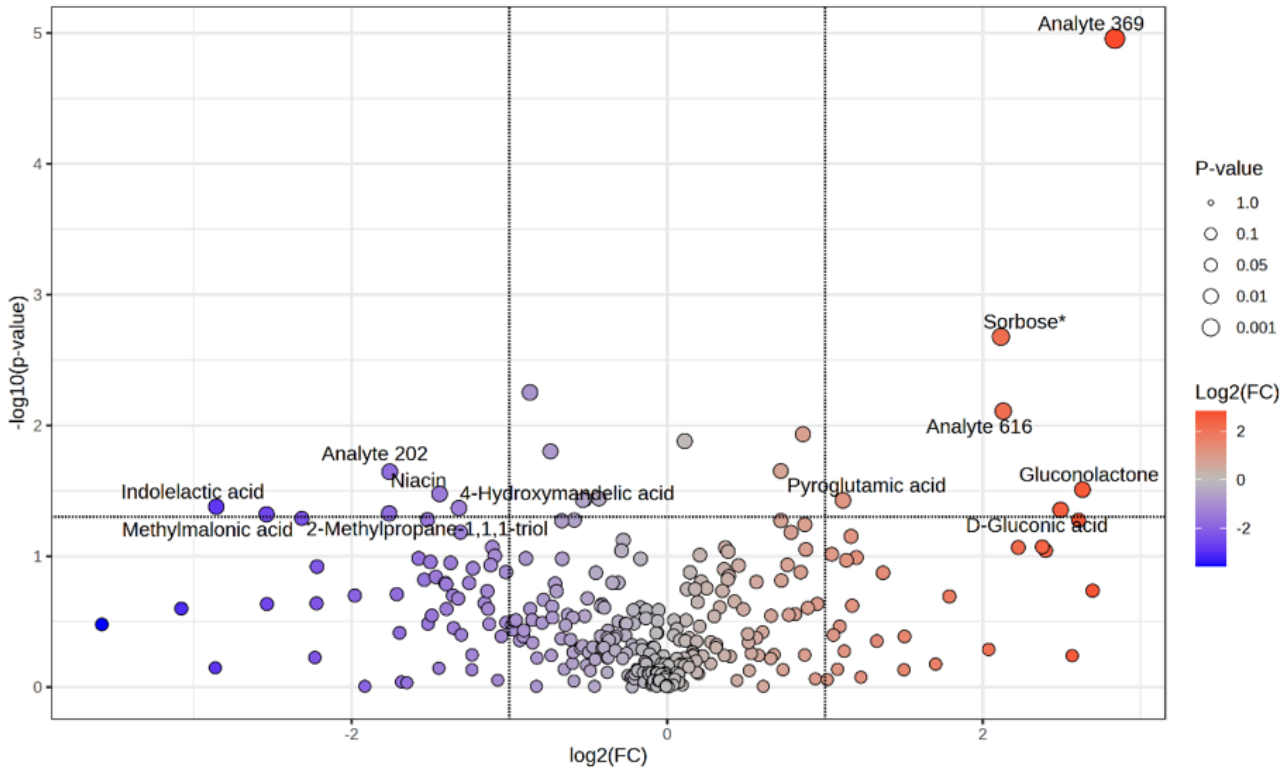


Figure 6

Volcano plot displaying the distribution of CSF metabolites according to their log_2 fold change (x-axis) and $-log_{10}$(p-value) (y-axis). Metabolites with a raw $p < 0.05$ and $FC \geq 2.0$ or $FC \leq 0.5$, are annotated, representing those significantly altered between positive and negative study groups.

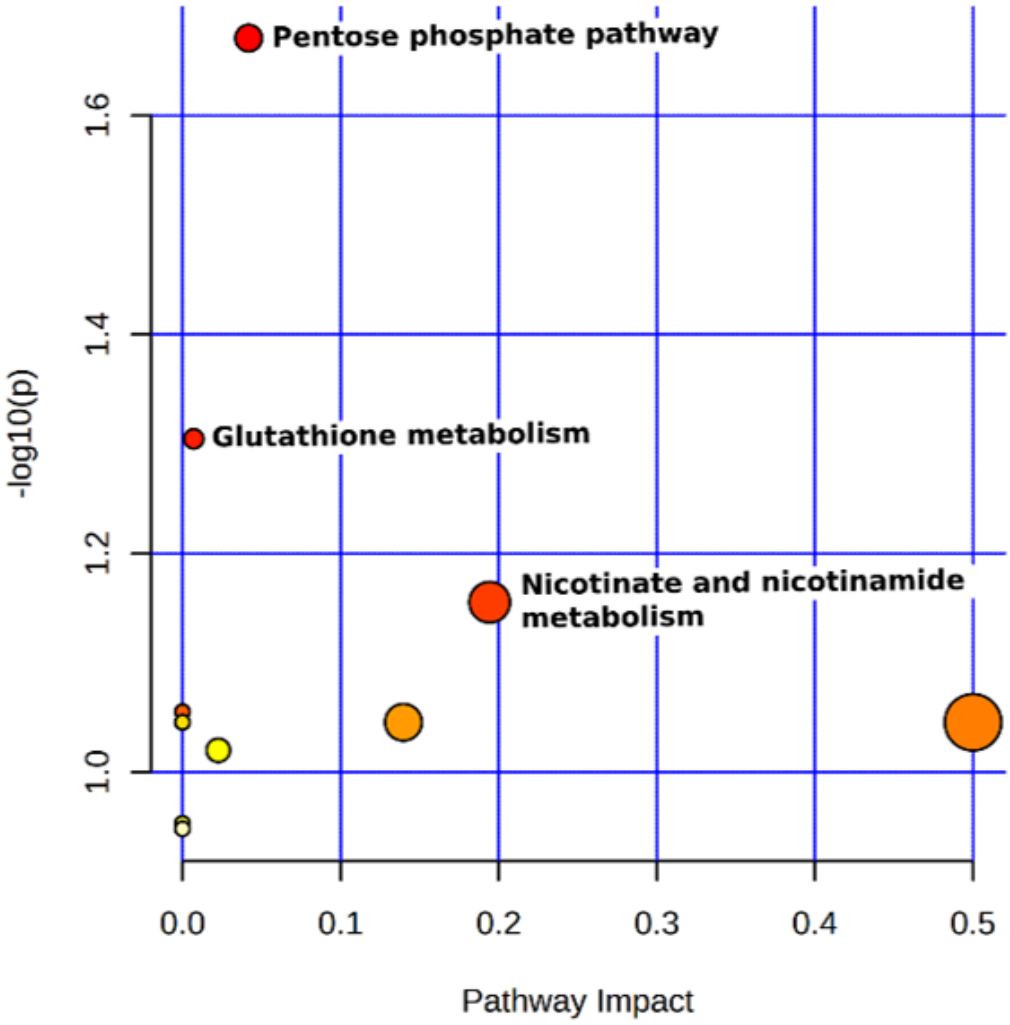


Figure 7

Pathway analysis of CSF metabolites identified from initial differential metabolite analysis. Pathways are ranked according to pathway impact (x-axis) and $-\log_{10}$(p-value) (y-axis), reflecting both the magnitude of metabolite enrichment and statistical significance. Larger and darker nodes indicate pathways with greater impact and significance. Annotated pathways represent those most affected between positive and negative study groups.

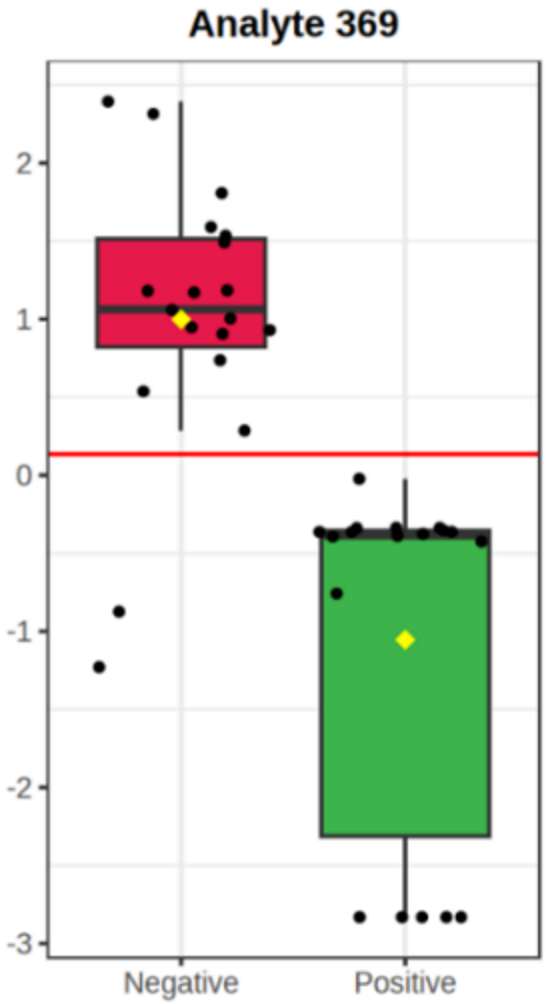


Figure 8

Box plot of Analyte 369, the CSF differential metabolite from ROC analysis. The red horizontal line denotes the optimal classification cutoff determined by the ROC model, representing the threshold value that best separates the two groups based on metabolite intensity.

Supplementary Files

This is a list of supplementary files associated with this preprint. Click to download.

- Supplementaryinformation.docx